Ammar TIBOUCHE[1], Kamel BOUDEGHDEGH[1]

University of Jijel Algeria (1)

Three-dimensional modeling of the magnetothermal phenomena by finite volume method - Application to the heating prior to deformation

***Abstract**. This paper presents a three-dimensional model of the magnetothermal phenomena in a transient thermal regime, for a quasi-homogeneous heating prior to deformation of the product under treatment. The aim of this work is to show the different parameters that influence this process during the transient heating to attain the desired final temperature. The electromagnetic and thermal phenomena are interdependent and strongly nonlinear.The Maxwell's equations and the thermal equation have been solved by Finite Volume Method.*

***Streszczenie.** W artykule zaprezentowano trójwymiarowy model zjawisk magneto termalnych w przejściowych warunkach termicznych, towarzyszących grzaniu quasi-homogenicznemu przy deformacji wstępnej obrabianej próbki. Celem pracy było wskazanie parametrów mających wpływ na ten proces do momentu osiągnięcia wymaganej temperatury. (**Trójwymiarowe modelowanie zjawisk magneto termalnych wykorzystujące metodę objętości skończonych - operacje grzania przy deformacji wstępnej**)*

Keywords: 3D magnetothermal simulation, transient thermal regime, finite volume method, prior deformation.
Słowa kluczowe: Symulacja magneto termalna 3D, przejściowe warunki termiczne, metoda objętości skończonych, deformacja wstępna

Introduction

Several studies have been devoted to the development of mathematical and numerical models for the magneto-thermal coupling. In [1, 2, 3], the authors use two-dimensional models fed by current and voltage, applied to induction heating system. In [4, 5], the authors present a three-dimensional magneto-thermal model, based on the finite element method.

In our paper, the numerical modeling of the provided induction heater for the treatment of product and for aim to obtain *a* quasi homogeneous temperature*,* several technical problems confront us:

The first problem is the development of three-dimensional magneto-thermal model [4, 5], but is based on the finite volume method (FVM). This method is very consistent to solving the thermal problems, and will be extended to that of the electromagnetic problem [6].

The second problem is related to the heater device. The induction heater is provided to treat bars of square section, in static and ensure a given production rate. The induction heater use multi-layer solenoid inductor. The mode stepper transfer of the bars is the type used, which it can be considered as a static heating [7].

The third problem is related to the development of the computer code of a three dimensional model of coupled phenomena.

Electromagnetic formulation

Neglecting the displacement currents, on a modified magnetic vector potential formulation for the three-dimensional with penalty term is given by the following electromagnetic equation [4, 8, 9] :

$$Rot\left(\frac{1}{\mu}rot\vec{A}\right)-gr\vec{a}d\left(\frac{1}{\mu}div\vec{A}\right)+\sigma\frac{\partial\vec{A}}{\partial t}=\vec{J}_s \quad (1)$$

where: σ – electrical conductivity, μ – magnetic permeability, J_s – coil current density.

The electrical conductivity and the magnetic permeability as function the temperature.

For the uniqueness of the solution, the Coulomb gauge is enforced in the system by introducing a penalty term to the equation (1). The boundary conditions at physical infinity are:

$$A=0 \quad (2)$$

Thermal formulation

The thermal equation in the transient regime is [10]:

$$\rho C_p\frac{\partial T}{\partial t}=div(K\,gr\vec{a}d(T))+P \quad (3)$$

with :

$$P=\frac{1}{2}\sigma\omega^2AA^* \quad (4)$$

The Boundary and Initial Conditions are given by specified temperature boundary condition, convection and/or radiation boundary condition:

$$T=T_0 \ or\ -K\frac{\partial T}{\partial n}=h_{eq}(T-T_a) \quad (5)$$

where: h_{eq} – the sum of the coefficients for convection and radiation exchange, T_a – ambient temperature.

Numerical magnetothermal model

The induction heating is governed by a system of nonlinear differential equations. A software tool on the base of the finite volume method has been developed.

These equations are integrated over each control volume, which in Cartesian coordinates is written ΔxΔyΔz (figure 1).

The heat conduction equation in Cartesian coordinates is given by :

$$\rho C_p\frac{\partial T}{\partial t}=\frac{\partial}{\partial x}\left(k\frac{\partial T}{\partial x}\right)+\frac{\partial}{\partial y}\left(k\frac{\partial T}{\partial y}\right)+\frac{\partial}{\partial z}\left(k\frac{\partial T}{\partial z}\right)+P \quad (6)$$

By integrating each term of this equation in space and time, we obtain for the first term of this equation (the same for the other terms):

$$\int_b^a\int_d^c\int_f^e\int_t^{t+\Delta t}\rho C_p\frac{\partial T}{\partial t}dxdydzdt=\Delta x\Delta y\Delta z\int_t^{t+\Delta t}\rho C_p\frac{\partial T}{\partial t}dt=\Delta x\Delta y\Delta z\rho C_p(T_p^{t+\Delta t}-T_p^t) \quad (7)$$

We finally obtain the expression for the temperature at any point (i, j, k) inside the study domain by using the implicit method:

$$T_{(i,j,k)}^{n+1}=\frac{1}{c_0}\begin{bmatrix}c_1T_{(i,j,k)}^{n}+c_2T_{(i+1,j,k)}^{n+1}+c_3T_{(i-1,j,k)}^{n+1}+\\c_4T_{(i,j+1,k)}^{n+1}+c_5T_{(i,j-1,k)}^{n+1}+c_6T_{(i,j,k+1)}^{n+1}+\\c_7T_{(i,j,k-1)}^{n+1}+P_{(i,j,k)}^{n}\Delta x_i\Delta y_j\Delta z_k\end{bmatrix} \quad (8)$$

(n+1) indicates the number of the iteration at the instant t=(n+1)Δt

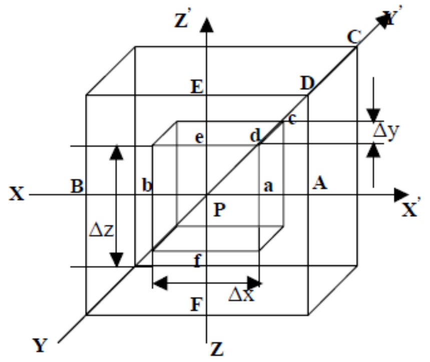

Fig.1. Control volume around the point p

The general magnetodynamic equation in Cartesian coordinates, without the gauge, is given by:

$$
(9)\qquad
\begin{aligned}
&\frac{\partial^2 A_x}{\partial y^2}+\frac{\partial^2 A_x}{\partial z^2}-\frac{\partial^2 A_y}{\partial x\partial y}-\frac{\partial^2 A_z}{\partial x\partial z}-j\sigma_\alpha\mu_\alpha\omega A_x=\mu_\alpha J_{sx}\\
&\frac{\partial^2 A_y}{\partial x^2}+\frac{\partial^2 A_y}{\partial z^2}-\frac{\partial^2 A_x}{\partial x\partial y}-\frac{\partial^2 A_z}{\partial y\partial z}-j\sigma_\alpha\mu_\alpha\omega A_y=\mu_\alpha J_{sy}\\
&\frac{\partial^2 A_z}{\partial x^2}+\frac{\partial^2 A_z}{\partial y^2}-\frac{\partial^2 A_x}{\partial x\partial z}-\frac{\partial^2 A_y}{\partial y\partial z}-j\sigma_\alpha\mu_\alpha\omega A_z=\mu_\alpha J_{sz}
\end{aligned}
$$

The index α indicates *the different regions of the domain* (inductor, air, load).

By integrating each term of these equations in space, we obtain for the first term of these equations (the same for the other terms):

$$
(10)\qquad
\begin{aligned}
&\int_b^a\int_d^c\int_f^e \frac{\partial^2 A_x}{\partial y^2}dxdydz=\Delta x\Delta z[(\frac{\partial A_x}{\partial y})_c-(\frac{\partial A_x}{\partial y})_d]=\\
&\frac{\Delta x\Delta z}{\Delta y}[A_{Ax}-2A_{px}+A_{Bx}]
\end{aligned}
$$

Finally, we obtain the final system to solve:

$$
(11)\qquad
\begin{aligned}
A_{x(i,j,k)}=&\frac{1}{a_{0(i,j,k)}}[a_{1(i,j,k)}J_{sx(i,j,k)}+\Delta z_k F_{1(i,j,k)}+\\
&\Delta y_j F_{2(i,j,k)}+a_{2(i,j,k)}(A_{x(i,j+1,k)}+A_{x(i,j-1,k)})+\\
&a_{3(i,j,k)}(A_{x(i,j,k+1)}+A_{x(i,j,k-1)})]\\
A_{y(i,j,k)}=&\frac{1}{b_{0(i,j,k)}}[b_{1(i,j,k)}J_{sy(i,j,k)}+\Delta x_i F_{3(i,j,k)}+\\
&\Delta z_k F_{4(i,j,k)}+b_{2(i,j,k)}(A_{y(i+1,j,k)}+A_{y(i-1,j,k)})+\\
&b_{3(i,j,k)}(A_{y(i,j,k+1)}+A_{y(i,j,k-1)})]\\
A_{z(i,j,k)}=&\frac{1}{c_{0(i,j,k)}}[c_{1(i,j,k)}J_{sz(i,j,k)}+\Delta x_i F_{5(i,j,k)}+\\
&\Delta y_j F_{6(i,j,k)}+c_{2(i,j,k)}(A_{z(i,j+1,k)}+A_{z(i,j-1,k)})+\\
&c_{3(i,j,k)}(A_{z(i+1,j,k)}+A_{y(i-1,j,k)})]
\end{aligned}
$$

with:

$$F_{1(i,j,k)}=A_{y(i+1,j-1,k)}+A_{y(i-1,j+1,k)}-A_{y(i+1,j+1,k)}-A_{y(i-1,j-1,k)}$$

$$F_{2(i,j,k)}=A_{z(i+1,j,k-1)}+A_{z(i-1,j,k+1)}-A_{z(i+1,j,k+1)}-A_{z(i-1,j,k-1)}$$

$$F_{3(i,j,k)}=A_{x(i+1,j-1,k)}+A_{x(i-1,j+1,k)}-A_{x(i+1,j+1,k)}-A_{x(i-1,j-1,k)}$$

$$F_{4(i,j,k)}=A_{z(i,j+1,k-1)}+A_{z(i,j-1,k+1)}-A_{z(i,j+1,k+1)}-A_{z(i,j-1,k-1)}$$

$$F_{5(i,j,k)}=A_{x(i+1,j,k-1)}+A_{x(i-1,j,k+1)}-A_{x(i+1,j,k+1)}-A_{x(i-1,j,k-1)}$$

The terms $a_{0\text{-}4(i,j,k)}$, $b_{0\text{-}4(i,j,k)}$, $c_{0\text{-}4(i,j,k)}$ are functions of the geometrical and physical parameters of the volume element (i, j, k).
Along the edge of the infinite domain, we take as the limit :

$$(12)\qquad A_{x(i,j,k)}=A_{y(i,j,k)}=A_{z(i,j,k)}=0+j0$$

The Coulomb gauge condition can be added numerically as penalty term in the equation system or as a separated equation from the system.

Magnetothermal coupling

If we consider the strong coupling between the equations, we would have obtained a system of equations to a single unknown X to seven (07) components for each volume element. The resolution of this system is possible [11], but it presents some numerical difficulties, because of the large matrix sizes and sometimes the definition of domains for some of components of the unknown X are mutually incompatible [12].

We therefore opted for a weak coupling. That is to say, that each system of equations is solved separately. However, we use the Gauss Seidel iterative method for the calculation process.

Application

In this application we are interested particularly to the heating of aluminum bars at 500 ° C. The phenomena of exchange with the ambient are present for all to the exterior surfaces. Numerically, we take: the coefficient of convection exchanges equal to *10 w/(m²·k)*, the emissivity equal to 0.8 (corresponds to $\varepsilon\sigma=4.5x10^8$ *w/(m²·k⁴)*). The induction heater is provided to treat the bars of square section for an inductor that suits their passage. We take as basic dimensions those of reference [13]: $L_x=L_y=80$ *mm*, The length of the inductor $L_{ind}=5.5$ *mm*, has 5 contiguous turns in which flows a current $I=I_s$ of 500 Hz. For our application the air gap thickness $L_e=10$ *mm*. However, one delimits the infinite box at $L_\alpha=100$ *mm* (10 times the thickness of the air gap and almost 20 times the length of the inductor). The length of the load is limited to this type of heater to that of the inductor ($L_z=5.5$ *mm*).

In the present work, our main concern is to obtain the desired temperature, for a quasi homogeneous distribution, without taking into account the heating time.

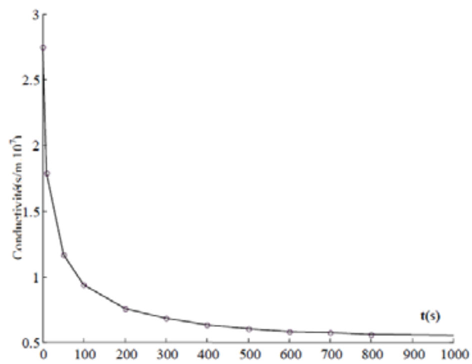

Fig.2. Evolution of the electrical conductivity

Variation of electrical conductivity with the temperature on the surface

The figure (2) shows the evolution of electrical conductivity on the surface (the plane $x=0$) of the center point. As the temperature increases it decreases rapidly at the starting of the heater and slowly by approaching to the permanent regime.

Evolution of the dissipated power

The increase of the electrical resistivity with the temperature which in turn leads to an increase in the depth of penetration causes a considerable drop in power at the starting of the heater (decrease by 50% after 20s). During the last phase of the heating, the sources of energies evolve slowly and the total power stabilizes to a value relatively weak regard to the one calculated to the initial temperature (599,78 W at 20°C). (Fig. 3)

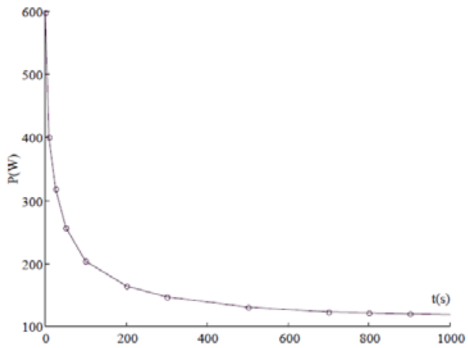

Fig.3. Evolution of the dissipated active power

Power density distribution along the x-axis

The curves are plotted at different times on the same line segment ($z=L_z/2$ and $y=L_y/2$) show that the power density distribution is qualitatively the same during the thermal transient regime (fig. 4). This power that is weak to the center of the load, increases progressively towards the outside of the side of the inductor. Finally, the evolution of the power is remarkable by a decrease enough high at the starting of the heater and weak to the last phase.

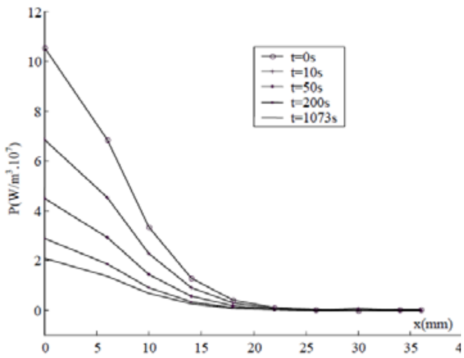

Fig.4. Power density distribution along the x-axis (central axis)

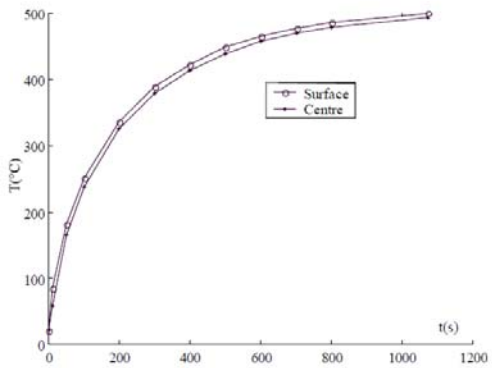

Fig.5. Evolution of temperature on the surface and the center

Evolution of temperature on the surface and the center

The figure (5) shows the evolution of the temperature at the center of the load and the center point of the surface (plane $x=0$). *During the heating process*, the two points qualitatively undergo the same variations: very quick at the beginning, average variation during the middle phase and almost constant at the end. For this application, the surface temperatures are always slightly higher than those of the center. This is justified by the fact that the load is a non-magnetic material and *the heat exchanges with the outside* remains low at this temperature (500°C).

Conclusion

A three-dimensional magnetothermal model of a induction heater was developed and tested. The heater is designed for heating static products prior to deformation. Through various simulations we find that power induced is strongly related to the intensity and frequency of the current. This power decreases progressively as the temperature increases. We are concluded that many parameters are involved in order to get the final desired temperature and a quasi homogenous distribution. These parameters are related to the working conditions and the nature of the material to be treated. This will allow us later to expand our work to a techno-economic study. We also note that it is fundamental to test and to verify that the margin of the power variation is sufficient to increase the temperature of the product from 20 to 500 ° C.

REFERENCES

[1] Louaayoua M., Naït- Saïd N., Louai F.Z., 2D finite element method study of the stimulation induction heating in synchronic thermography NDT, *NDT & E Int.*, vol. 41 (2008), 577-581

[2] TIBOUCHE A., MEKIDECHE M. R., DJERDIR A., MIRAOUI A., The Mixed Method Modeling of the Transient Electro-Magneto-Thermal Phenomena Fed by Voltage and Current, *Acta Electrotehnica*, Vol. 46 (2005), No. 4, 159-167

[3] Rumena S., Ilona I., Ilonka L., Hristophor T., Coupled field induction heating system, *Przeglad Elektrotechniczny*, 11 (2007), .201-203

[4] Mimoune S.M., Fouladgar J., Develey G., Modeling of 3D electromagnetic and heat phenomena for materials with poor conductivity, *IEEE Trans. Magn.*, 31 (1995), No. 6, 3578-3580

[5] LOUAI F.Z., Modèles magnétodynamiques d'éléments finis pour structures tridimensionnelles de chauffage par induction, *Thèse de doctorat*, Ecole centrale de Nantes, France, 1995

[6] Patankar S.V., Numerical heat transfer and flow fluid, *Mc. Graw Hill*, 1979

[7] TOURAINE A., Applications du réchauffage par induction lors de la transformation des métaux, *Techniques de l'ingénieur – réchauffage par induction*, Fiche M 712, 1-12

[8] GUERIN C., MARECHAL Y., MEUNIER G., Numerical aspects of 3D magnetodynamic formulations using the magnetic vector potential, *IWEMF*, Belgique, septembre 1992

[9] BIRO O., PREIS K., On the use of the magnetic vector potential in the finite element analysis of three-dimensional eddy currents, *IEEE Trans. Magn.*, 25 (1989), No. 4, 3145-3159

[10] Mei R.B., Li C.S., Liu X.H., Han B., Analysis of strip temperature in hot rolling process by finite element method, *Journal of Iron and Steel Research*, International, 17 (2) (2010), 17–21

[11] FELIACHI M., DEVELY G., Magneto-thermal behaviour Finite element analysis for ferromagnetic materials in induction heating devices, *IEEE Trans. Magn.*, 27 (1991), No. 6, 5235-5237

[12] MEKIDECHE M.R., Contribution à la modélisation numérique de torches de plasma d'induction, *Thèse de doctorat*, Ecole centrale de Nantes, France, 1993

[13] Froehlich R., Application de l'électricité dans les procédés industriels, *DOPEE*, 85 (1987)

***Authors**: prof. (Asso.) Ammar Tibouche, Department of Electrical Engineering, Jijel University, B.P 98, Jijel, Algeria, E-mail: Tibouche_ammar@yahoo.fr; dr Kamel Boudeghdegh, Department of Chemical Engineering, Jijel University, B.P 98, Jijel, Algeria, E-mail: Kameltan@yahoo.com.*